ELSEVIER

Fluid Phase Equilibria 150–151 (1998) 83–90

FLUID PHASE EQUILIBRIA

Hydrophobicity in a simple model of water: solvation and hydrogen bond energies

K.A.T. Silverstein [a], K.A. Dill [b], A.D.J. Haymet [c,*,1]

[a] *Graduate Group in Biophysics, University of California, San Francisco, CA 94143-1204, USA*
[b] *Department of Pharmaceutical Chemistry, University of California, San Francisco, CA 94143-1204, USA*
[c] *School of Chemistry, University of Sydney, Sydney, NSW 2006, Australia*

Abstract

We explore a simple model of water: Lennard–Jones disks in two dimensions, subject to a Gaussian orientation-dependent hydrogen-bond function. The model, originally developed by Ben-Naim, shows the anomalous features of water and aspects of the hydrophobic effect. Here we further explore its phase diagram and related properties by NPT Monte Carlo simulations. © 1998 Elsevier Science B.V. All rights reserved.

Keywords: Hydrophobicity; Phase diagram; Two dimensions; Water model

1. Introduction

We explore the properties of a simple model of water, proposed originally by Ben-Naim [1,2]. We have found, through NPT Monte Carlo simulations, that this model qualitatively reproduces several anomalous trends of water, including the density anomaly, a negative thermal expansion coefficient at low temperature, the large heat capacity of the condensed phase, a minimum in the isothermal compressibility as a function of temperature, and the proper temperature trends of the thermodynamics of hydrophobic transfers [3].

The model, which we call MB water (because of its resemblance to the Mercedes–Benz logo) represents water molecules as standard Lennard–Jones (LJ) disks in two dimensions with three symmetrically-arranged arms. The arms attract each other through an explicit hydrogen-bonding (HB) interaction.

* Corresponding author.
[1] Present address. Department of Chemistry and Institute for Molecular Design, University of Houston, Texas 77204.

0378-3812/98/$ - see front matter © 1998 Elsevier Science B.V. All rights reserved.
PII: S0378-3812(98)00278-7

The potential of interaction between two water molecules is defined by two terms:

$$U(\boldsymbol{X_i}, \boldsymbol{X_j}) = U_{LJ}(r_{ij}) + U_{\mathrm{HB}}(\boldsymbol{X_i}, \boldsymbol{X_j}), \tag{1}$$

where, using Ben–Naim's original notation, $\boldsymbol{X}_i$ denotes the vector representing both the coordinates and the orientation of the ith particle, and r_{ij} is the distance between the molecular centers of particles i and j. The LJ term is customarily written as

$$U_{\mathrm{LJ}}(r_{ij}) = 4\epsilon_{\mathrm{LJ}}\left[\left(\frac{\sigma_{\mathrm{LJ}}}{r_{ij}}\right)^{12} - \left(\frac{\sigma_{\mathrm{LJ}}}{r_{ij}}\right)^{6}\right], \tag{2}$$

where ϵ_{LJ} and σ_{LJ} are the well-depth and contact parameters, respectively.

The hydrogen bond is defined to be optimal at a specified distance and relative orientation of the two participating molecules:

$$U_{\mathrm{HB}}(\boldsymbol{X}_i, \boldsymbol{X}_j) = \epsilon_{\mathrm{HB}} G(r_{ij} - r_{\mathrm{HB}}) \sum_{k,l=1}^{3} G\left(\hat{\boldsymbol{i}}_k \cdot \hat{\boldsymbol{u}}_{ij} - 1\right) G\left(\hat{\boldsymbol{j}}_l \cdot \hat{\boldsymbol{u}}_{ij} + 1\right). \tag{3}$$

In this expression, the minimum energy ϵ_{HB} corresponds to an idealized hydrogen bond configuration in which one arm of molecule i aligns with an arm of molecule j, and the two molecules' centers are separated by a distance r_{HB}. The unit vector $\hat{\boldsymbol{i}}_k$ represents the kth arm of the ith particle ($k = 1, 2, 3$) and $\hat{\boldsymbol{u}}_{ij}$ is the unit vector joining the center of molecule i to the center of molecule j. The parameters $\epsilon_{\mathrm{HB}} = -1$ and $r_{\mathrm{HB}} = 1$ define the optimal hydrogen bond energy and bond length, respectively. Deviations from this lowest-energy hydrogen-bond configuration (in relative interparticle separation or angle) are described by the unnormalized Gaussian function, $G(x)$, with a single width parameter, σ, for all degrees of freedom:

$$G(x) = \exp\left[-x^2/2\sigma^2\right]. \tag{4}$$

All energies and temperatures are reported in reduced units, normalized to the strength of the optimal hydrogen bond, $|\epsilon_{\mathrm{HB}}|$ (e.g., $T* = k_{\mathrm{B}}T/|\epsilon_{\mathrm{HB}}|$, $H* = H/|\epsilon_{\mathrm{HB}}|$). Likewise all distances are scaled by the length of an idealized hydrogen bond separation, r_{HB} (e.g., $V* = V/r_{\mathrm{HB}}^2$). The interaction energy, ϵ_{LJ} is one-tenth of ϵ_{HB}, and the LJ contact distance is 0.7 that of r_{HB}. The width of the Gaussian is $\sigma = 0.085$.

To obtain thermodynamic and structural properties of MB water, we performed Monte Carlo simulations in the NPT ensemble [4] on systems of 60 water molecules, using standard periodic boundary conditions and the minimum-image convention. The first 1×10^6 configurations were discarded after a random initial state chosen at each phase point. Nonpolar solutions were performed with 60 water molecules and a single LJ solute (with the same ϵ_{LJ} and σ_{LJ} values as their water counterparts) fixed in the center of the simulation box.

More details on the model and simulation procedures may be found in the original papers [1,2] and Refs. [3,5]. We further explore some macroscopic and microscopic properties of MB water in Sections 2 and 3.

2. Phase diagram

In addition to the properties mentioned above, MB water shows some other similarities to real water. We display a rough P–T phase diagram in Fig. 1. The solid/liquid and solid/gas boundaries

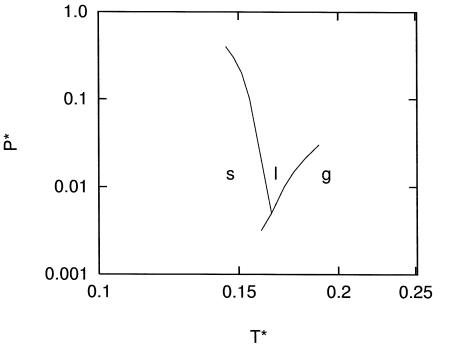

Fig. 1. Rough sketch of the $P-T$ phase diagram (log–log plot). The labels s, l, and g denote the solid, liquid, and gas phase regions, respectively. The high temperature end of the gas liquid line is our estimate for the critical point. Reduced temperature is normalized by the optimal hydrogen bond energy ($T* = k_B T/\epsilon_{HB}$). Pressure is defined such that $P*V* = PV/|\epsilon_{HB}|$ (where $V* = V/r_{HB}^2$).

were determined by locating the large jump in the heat capacity when slowly raising the temperature from an initial ice configuration (with long equilibration times between temperatures). The liquid/gas boundaries were determined from the method of Hansen and Verlet [6]. The most notable property of this sketch is the negative slope of the liquid–solid coexistence line. Water is among the few substances which have this property.

3. Details of hydrogen bonding

Fig. 2 shows the centers pair correlation function, $g(r)$, at several temperatures. The first shoulder occurs at the characteristic van der Waals distance of the model. The primary and subsequent peaks occur at the first, second, third, etc., hydrogen-bond neighbor distances. A pronounced breakdown in structure is observed with temperature.

Some insight into a possible molecular cause of the density anomaly may be obtained by tracking some other structural features. The density anomaly appears to arise from a two-part mechanism. Initially, ice has a very open hydrogen-bonded structure. Upon melting, however, some of these hydrogen bonds (HB) are weakened or broken, and replaced with more dense-packing van der Waals

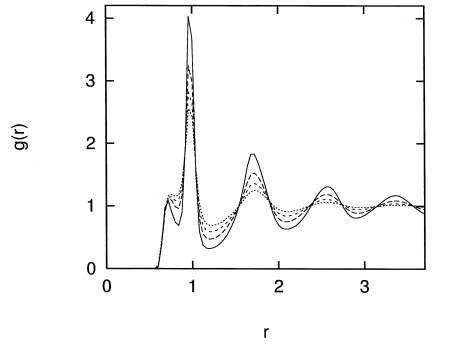

Fig. 2. Pair correlation function for pure MB water at four temperatures: $T* = 0.16$ (solid), $T* = 0.20$ (large-dashed), $T* = 0.24$ (small-dashed), and $T* = 0.28$ (dotted).

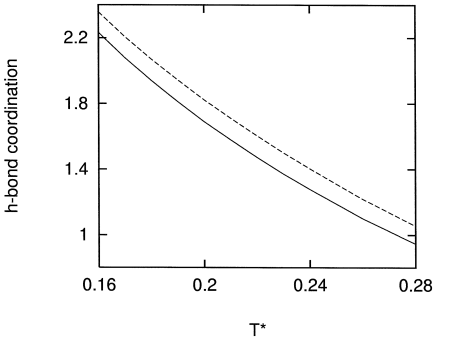

Fig. 3. Average hydrogen-bond coordination of bulk water molecules vs. temperature using a cutoff of −0.5 (solid line) and −0.4 (dashed line).

(VDW) interactions. This process of exchanging open HB arrangements for more-compact and higher-energetic VDW interactions continues in the fluid until thermal fluctuations begin to drive the molecules apart once the temperature of maximum density (TMD) is passed (the TMD in this model occurs at $T* = 0.18$).

Evidence supporting this explanation can be obtained by tracking the distributions of HB and VDW coordination of the water molecules. To do this, we assign an arbitrary energetic cutoff. If the HB or VDW energetic terms are below the cutoff in a pairwise interaction, then each of the molecule's corresponding coordination counters is incremented. The cutoffs (−0.5 for HB, and −0.06 for the VDW), correspond to minima in the pair interaction energies. The minimum that corresponds to the HB cutoff is quite broad (it is roughly level from −0.5 to −0.3), and hence the trends in HB coordination are fairly insensitive to the cutoff value. The average HB coordination starts out quite high in the low-temperature fluid, and steadily decreases with temperature, as can be seen in Fig. 3. In contrast, the minimum corresponding to the VDW cutoff is very sharp, and more lenient cutoffs can change the VDW counting considerably. This is partly because the very weakest VDW interactions overlap to some degree with corresponding hydrogen-bonding distances. Fig. 4 shows that initially the number of strong VDW contacts increases and then levels off before decreasing. Weaker VDW contacts diminish after the TMD.

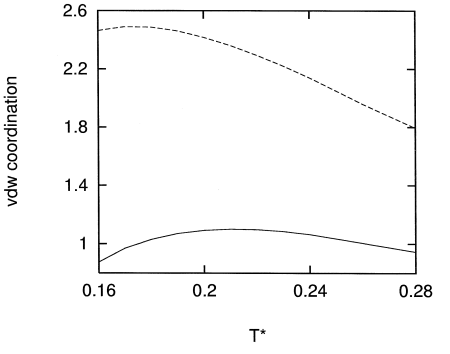

Fig. 4. Average VDW coordination of bulk water molecules vs. temperature using a cutoff of −0.06 (solid line) and −0.04 (dashed line).

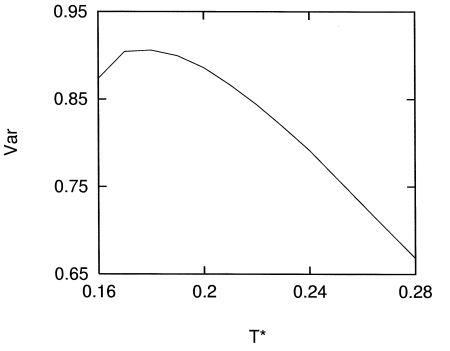

Fig. 5. Variance in the hydrogen-bond coordination of bulk water molecules vs. temperature (cutoff of -0.5).

The exchange of HB and VDW contacts leads to restructuring in the fluid. Hence, the variance in the distribution of HB coordinations is quite high, peaking at the TMD (see Fig. 5). This is consistent with the explanation of Stillinger [7] of the density anomaly, in which compression arises from the

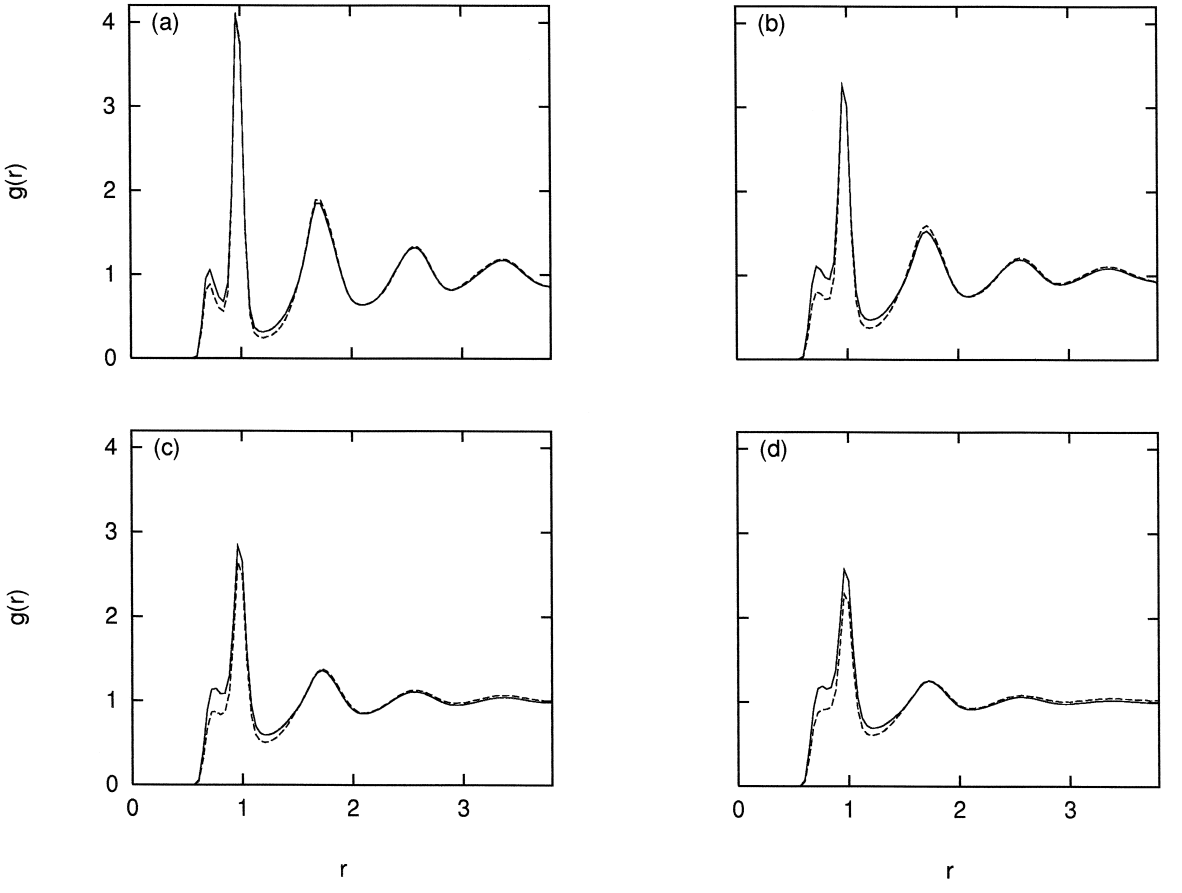

Fig. 6. Water–water pair correlation function at four temperatures: (a) $T* = 0.16$, (b) $T* = 0.20$, (c) $T* = 0.24$, and (d) $T* = 0.28$ for shell water molecules (dashed) and bulk (solid) water molecules.

shift from ice-like six-membered hydrogen-bonded rings towards more and more strained hydrogen-bonded ring networks.

It is possible that the minimum in the compressibility arises from the same balance of VDW and HB interactions. The initial increase in VDW contacts crowds the local molecular environment to some degree, making the fluid less compressible. Then, as the number of bent or broken hydrogen-bonds becomes appreciable, the fluid ultimately increases its compressibility.

The microscopic origins of the hydrophobic effect have long been under debate. One group [8–10] holds that hydrophobicity results mostly from the small size of the water molecule, and not from water structuring by the solute. Much of this argument may simply be semantic [11–13]. We believe that the large positive heat capacity of insertion of nonpolar solutes is the defining feature of hydrophobicity. The present model suggests water structuring gives rise to the heat capacity. The issue is whether the water molecules at the solute surface change their degree of ordering differently than bulk water molecules with temperature. Figs. 6 and 7 show that they do.

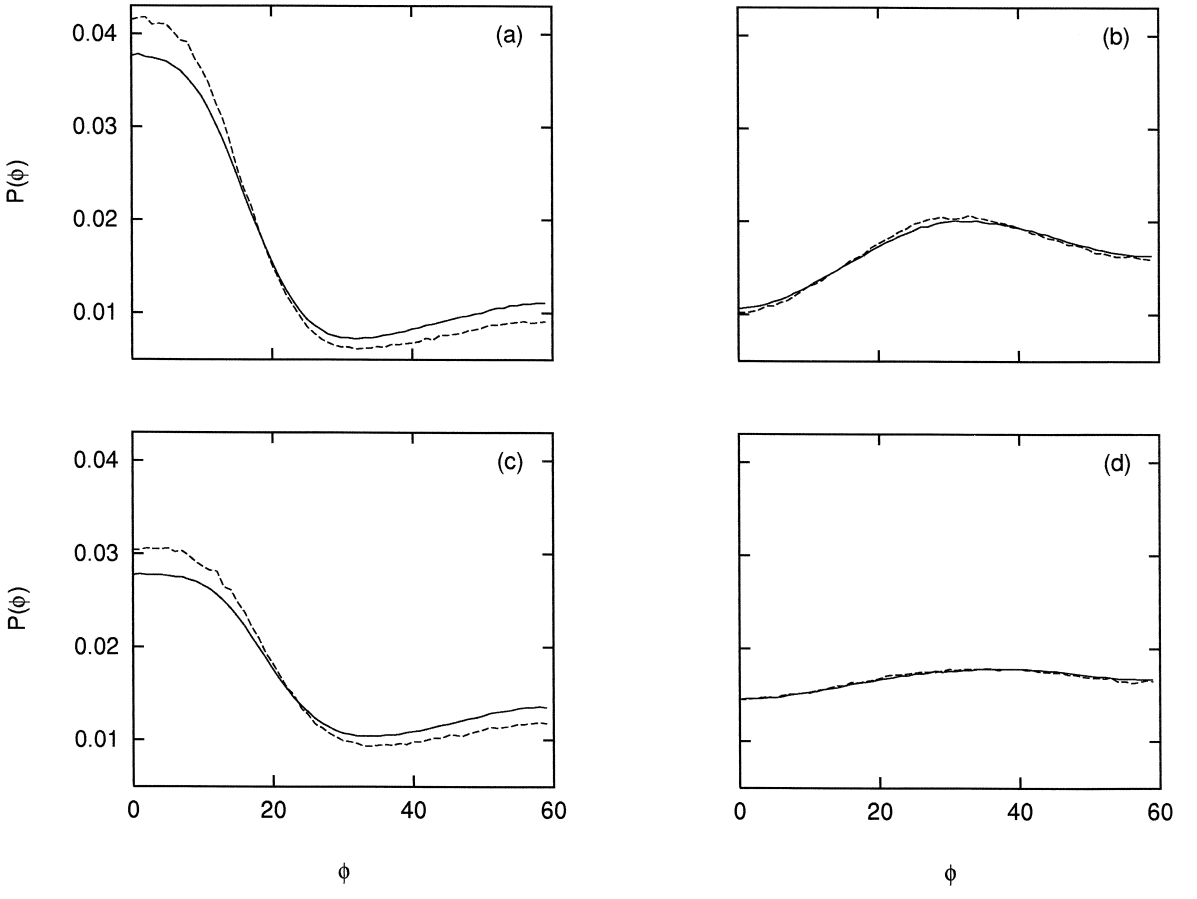

Fig. 7. Angular distributions of neighboring water molecules around shell (dashed) and bulk (solid) water molecules at two temperatures: (a) first neighbors, $T* = 0.16$; (b) second neighbors, $T* = 0.16$; (c) first neighbors, $T* = 0.24$; (d) second neighbors, $T* = 0.24$.

We define the first-shell water molecules as those within a given cutoff-distance from the solute (taken to be the first minimum in the solute–water pair correlation function). At low temperature, the water–water pair correlation, $g_{WW}(r)$, for the first-shell water molecules is remarkably similar to that of bulk water, despite the presence of the nearby solute (see Fig. 6). Only the VDW peak at a distance of ≈ 0.8 is diminished relative to the bulk counterpart. Then at higher temperature, the first hydrogen-bonding peak of the shell molecules becomes weaker than the corresponding bulk-water peak. The first and second neighbors, respectively, of bulk and shell water molecules are defined as those within the first and second minima of $g_{WW}(r)$. The angular distributions of water molecules in each of these categories are shown in Fig. 7 at several temperatures. We find that at all temperatures studied, the first-neighbors of shell molecules have more orientational order than those about bulk water molecules. Second-neighbors to shell water molecules only show enhanced ordering at lower temperatures.

4. Conclusions

In this work we have further evaluated the MB model of water, and have investigated finer structural rearrangements with increasing temperature. We find that MB water captures qualitatively the correct trends of the $P–T$ phase diagram.

The density anomaly arises in the model from a balance of two factors: the close-packed van der Waals contacts are pitted against more open hydrogen-bonded interactions. By tracking the average hydrogen-bond and van der Waals coordination of water molecules, we observe that hydrogen bond interactions are replaced with van der Waals contacts up to the temperature of maximum density (TMD). Beyond that temperature, both types of contacts decrease, due to increased thermal fluctuations that expand the fluid.

Finally, in the case of hydrophobic solute transfers, we find that the structure of water molecules in the first and second hydration shells is more temperature sensitive than the structure of bulk water. These trends contribute to the temperature dependence of the transfer thermodynamics that characterize hydrophobicity in the MB model.

Acknowledgements

KATS gratefully acknowledges support under a U.S. National Science Foundation Graduate Research Fellowship and a UCSF Regent's Fellowship. In Australia this research was supported by the Australian Research Council (ARC) (Grant No. A29530010), and SydCom the USyd/UTS Distributed Processing Facility funded by an ARC infrastructure grant.

References

[1] A. Ben-Naim, J. Chem. Phys. 54 (1971) 3682.
[2] A. Ben-Naim, J. Chem. Phys. 59 (1973) 6535.
[3] K.A.T. Silverstein, A.D.J. Haymet, K.A. Dill, J. Am. Chem. Soc. 120 (1998) 3166.

[4] M.P. Allen, D.J. Tildesley, Computer Simulation of Liquids, Oxford Univ. Press, Oxford, 1987.
[5] A.D.J. Haymet, K.A.T. Silverstein, K.A. Dill, in: International Symposium on Molecular Thermodynamics and Molecular Simulation, Hosei University, Tokyo, Japan, 1997, pp. 143–152.
[6] J.-P. Hansen, L. Verlet, Phys. Rev. 184 (1969) 151.
[7] F.H. Stillinger, Science 209 (1980) 451.
[8] B. Lee, Biopolymers 24 (1985) 813.
[9] B. Lee, Biopolymers 31 (1991) 993.
[10] W. Blokzijl, J.B.F.N. Engberts, Angew. Chem., Int. Ed. Engl. 32 (1993) 1545.
[11] K.A. Dill, Science 250 (1990) 297.
[12] A.D.J. Haymet, K.A.T. Silverstein, K.A. Dill, Faraday Disc. 103 (1996) 117.
[13] D.E. Smith, A.D.J. Haymet, J. Chem. Phys. 98 (1993) 6445.